

Shaking Table Tests of Dou-gong Brackets on Chinese Traditional Wooden Structure: A Case Study of Tianwang Hall, Luzhi, and Ming Dynasty

Zherui Li,^{a,b} Yilin Que,^c Xiaolan Zhang,^{a,b} Qicheng Teng,^{a,d} Tongyu Hou,^a Yifan Liu,^a Xinmeng Wang,^a Zeli Que,^{a,*} and Kohei Komatsu^{a,b}

Using the Dou-gong brackets on the column of the Tianwang Palace in the Baosheng Temple from the Ming Dynasty as the research object, an experimental study was conducted on 15 groups of shaking table tests of a full-scale Dou-gong specimen made of Douglas fir. Through the analysis of dynamic magnification coefficient trends, the process of displacement characteristics of the Dou-gong in response to changes of vibration, and the rotary and sliding displacement values for each part of the Dou-gong at the largest deformation moments, major conclusions were drawn as follows. A higher vibration excitation intensity input resulted in a stronger damping effect of the Dou-gong model. The maximum deformation of each member had a strong correlation with the maximum deformation of the whole structure, among which the rotary deformation of the Lu-dou and Hua-gong occupied a dominant position. The Hua-gong with Ang, one special part of the Dou-gong, had relatively weak connection nodes during the tests; therefore more attention and relevant reinforcement measures should be taken on this part in the maintenance and conservation of cultural relics.

Keywords: Dou-gong; Chinese wooden structure; Anti-seismic performance; Shaking table test

Contact information: a: College of Materials Science and Engineering, Nanjing Forestry University, Nanjing, 210037, China; b: Research Institute for Sustainable Humanosphere, Kyoto University, Uji; 6110011, Japan; c: High School Affiliated with Nanjing Normal University, Nanjing, 210037, China; d: Baogوسي Ancient Architecture Museum, Ningbo, 315033, China;
* Corresponding author: zeliq@njfu.edu.cn

INTRODUCTION

As one of the world's three major architectural systems, Chinese ancient architecture plays an important role in the global history of architecture. With its long history, unique systematic features, and wide-spread employment, as well as its abundant heritages, Chinese ancient architecture keeps growing and developing. Emerging from a system using rammed earth (as ground work and wall) and wood to one using brick and wood, it held on to its tradition of using a wooden source as the main structure and carpentry as the main methodology. One of the most significant features of the traditional Chinese wooden structure is that it emphasizes the cross-section of structural members rather than joints, and insufficient horizontal connection is set between columns. So the mechanical properties of connection joints, especially the joints on the top of columns are the weak link on the anti-lateral performance of the whole building.

The Dou-gong bracket, a special connection component between the column and beam, plays a pivotal role in both structural force transmission and decorative function. Composed of many cantilever joists, named Gong, stacked one on top of another in a criss-

crossed pattern, and connected by Dou members, the Dou-gong bracket as a whole could be regarded as a pad supported at the end of a beam. This special structure functions as an inverted fixed-hinged support that has compression deflection and rotary movement on the vertical plane as well as slip movement on the horizontal plane (Pan 2008). With respect to the structural performance, because of the overhanging in two directions, the Dou-gong bracket shortens the span and enhances the load carrying capacity of the upper beams, which helps adjust the depth of the eaves, making them more graceful and harmonious. In contrast, instead of sticking together, all of the Dou and Gong components are connected by mortise and tenon joints. With the addition of its unique shape with overlapping cantilevers, the Dou-gong bracket becomes a ductile connection to dissipate energy between the column and beam, especially under lateral forces in earthquakes.

The study of significance to the modern world in the field of Chinese traditional wooden buildings started in the 1920s and 1930s (Liang 1934; Chen *et al.* 2012). Historic and artistic fields of architecture attracted the most attention and were often selected as the main research focus over a long period of time. In recent years, the outstanding anti-seismic property of the traditional wooden structure has attracted much attention. A few researchers selected the Yingxian wooden tower (Li *et al.* 2004; Yuan *et al.* 2011) and the main palace of the Forbidden City (Zhou *et al.* 2013, 2015) as objects, or made the Dou-gong and frame models based on two standards inherited both from the Song Dynasty (1103 A.D.) and the Qing Dynasty (1734 A.D.) (Fang *et al.* 1992; Gao *et al.* 2003), to test the static and dynamic behaviors. Some mechanical models of specific historical wooden buildings were established to prevent earthquake-inflicted damages. Until now, a limited number of fundamental studies have been conducted on the structural behavior of Chinese traditional wooden structure, especially on its typical joint connections. Furthermore, material performance and structural behavior research of Chinese traditional wooden buildings is often based on specific emergency repair and strengthening projects of historical buildings, without further study after the project finished, which somewhat limits the systematizations and universality of the research.

Concerning the Dou-gong bracket, existing domestic research studies mainly have focused on the forms of the Song Dynasty and the Qing Dynasty (Fang *et al.* 2009; Shao *et al.* 2014); the other forms in the transition period are often neglected. As a part, instead of an independent unit in the experiment, the Dou-gong brackets are often simplified as symmetric models with a reduced scale, which is vastly different from the reality. In addition, the above-mentioned anti-seismic behavior experiments and analyses are conducted with little reference to material properties. This paper uses the Dou-gong bracket of the Tianwang hall in the Baosheng temple in Luzhi, from the Ming Dynasty, as the research object, and refers to the analytical method of Hideo Kyuke (Kyuke *et al.* 2008). Full-scale shaking table tests of the Dou-gong model made of Douglas fir were conducted to explore the dynamic behavior of the whole structure, the deformation of the different layers, and the weak spots of the model.

EXPERIMENTAL

Materials

The full-scale configuration of the Dou-gong specimen used in this study followed that of the top of the column in the Tianwang Hall of the Baosheng temple (Suzhou, China). Tianwang Hall, verified to be reconstructed in the late Ming Dynasty (1630 A.D.) (Chen

1955), is the front hall of the Baosheng temple that stretches 11 meters from east to west and 7 meters from south to north, and has a Xieshan style roof with a single layer of eaves, as shown in Fig. 1.



Fig. 1. Tianwang Hall and its typical Dou-gong bracket on top of the column

The Dou-gong bracket on top of the column has three layers, the Lu-dou component on the bottom has a special round shape, and the Hua-gong with an Ang component on the second layer could be considered as a partial heritage structure from the Song Dynasty. Instead of using the Ang to support the purlin and roof load directly, this component changes the last part into the Hua-gong to support the beam and helps form a beam-column frame. Detailed names and positions of each component are shown in Fig. 2.

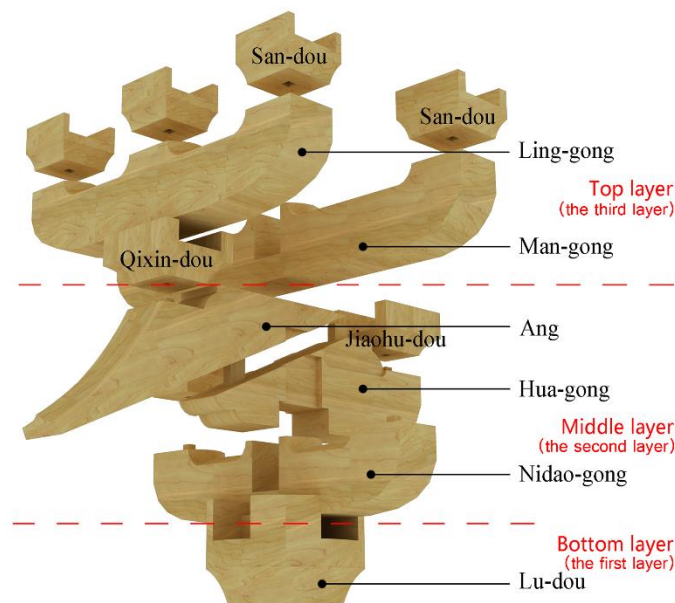


Fig. 2. The components and connections of the Dou-gong specimen

According to textual research, the original Dou-gong brackets in the Tianwang Hall were made of China fir (*Cunninghamia lanceolata*). Under clause 6.3.1 of GB/T 50165 (1992), if load-carrying members need to be restored or changed, the alternative materials

should stay the same as the original material. If this proves difficult, the alternative wood species' mechanical properties should be no less than that of the original. Considering the property differences between the old China fir and modern fast-growing timber materials, the Douglas fir (*Pseudotsuga menziesii*) was chosen to make the Dou-gong specimen. The detailed contrasts of basic mechanical properties between the test specimen material and the fast growing China fir are shown in Table 1.

Table 1. Mechanical Properties of Materials

Tree Species	Moisture Content (%)	Compressive Strength Parallel to Grain (MPa)		Bending Strength (MPa)		Elasticity Modulus (MPa)	
China fir	11.0	44.9 ± 1.4 *	41.8 **	55.6 ± 3.5	53.4	5601.7 ± 52.1	5517.7
Douglas fir	13.4	47.1 ± 3.6	50.4	75.9 ± 4.6	80.2	7153.1 ± 75.2	7303.3

Note: * standard deviation; ** modification value under moisture content of 12%

Methods

The dimensions of the final test specimen were 980 mm × 1050 mm × 613 mm, and the model weighed 48.9 kg. Specific sizes of their sub-units are shown in Table 2. The jointing design mainly included straight tenon joints and wooden dowel connections, while the Lu-dou component on the bottom was fixed on the shaking table by an iron hoop. Two purlins and a board were placed on the top layer of the Dou-gong bracket to make it level and add weight. Due to on-site facility limitations, the total vertical load was approximately 45 kg, mainly to keep the balance in the tests.

Table 2. Major Scantlings of the Dou-gong Specimen

Component Name	Length (mm)	Width (mm)	Height (mm)
Lu-dou	330	330	210
Hua-gong	615	110	180
Ang	600	110	285
Nidao-gong	730	110	165
Man-gong	1050	110	165
Ling-gong	805	110	165
Jiaohu-dou	195	195	100
San-dou	140	140	100

The aim of this shaking table test is to understand the dynamic structural behavior of the Dou-gong bracket and its sub-units under different vibration forms. Due to limitations of equipment, only the sinusoidal wave could be exported. Hence, instead of inputting vibration waves directly, similar accelerations were achieved *via* controlling different steps of vibration frequency and amplitude in 15 conditions. Figure 3 shows an overview of the model on the shaking table. The frequency input subsequently increased from 10 Hz to 15 Hz, 20 Hz, 25 Hz, and 30 Hz (corresponding actual frequencies were 1.05 Hz, 1.59 Hz, 2.10 Hz, 2.65 Hz, and 3.12 Hz), whereas the amplitude increased from 10 mm to 20 mm and 30 mm. The vibration direction was along the direction of the Hua-gong and Ang component, as shown in Fig. 4. The test time was controlled to 30 s, which was determined based on the characteristic frequency and amplitude of the El-centro seismic wave (Fan *et al.* 2008). The test number was comprised of the material (D means Douglas fir), input frequency, and amplitude.

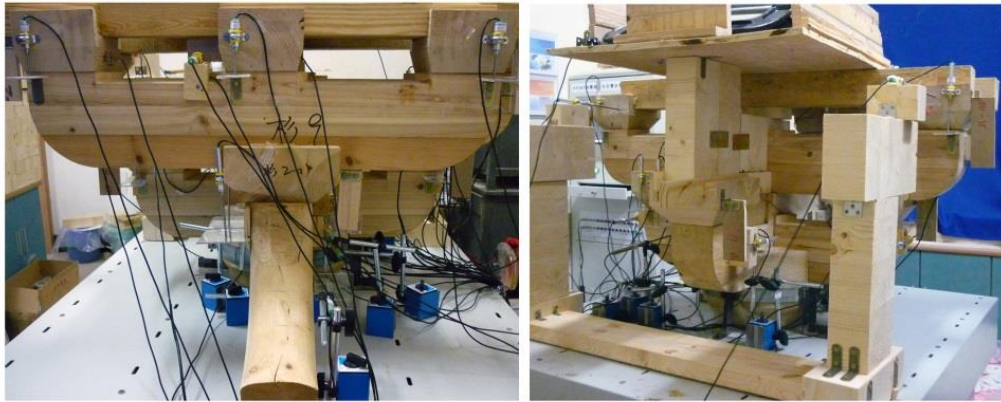


Fig. 3. The Dou-gong specimen fixed on the shaking table

The major equipment included a vibration table with four degrees of freedom (HPDZ-1; Nanjing Hope Tech. Co., Ltd., Nanjing, China) and a dynamic signal collection and analysis system (HPU100-F; Nanjing Hope Tech. Co., Ltd., Nanjing, China). A total of 41 channels of data were collected from the test, of which 39 displacement transducers and two accelerometers were used. The displacement transducers were assigned to measure the horizontal and vertical deflection of the adjoining Dou-gong members, relative displacement between each level, and absolute displacement of each level to the shaking table. Accordingly, both the sliding displacement and rotary displacement can be obtained through superposition. Two accelerometers were placed at the top and bottom of the specimen to record the acceleration response along the vibration axis direction. An overview of the positions of all the measuring devices is presented in Fig. 4.

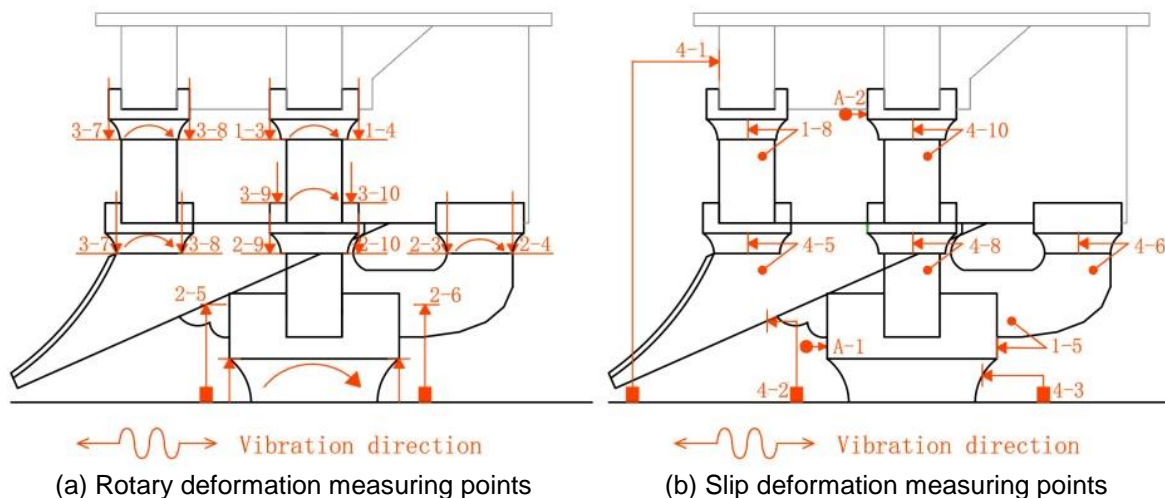


Fig. 4. Arrangement of measuring devices

RESULTS AND DISCUSSION

As a whole, the vibration characteristics of the Dou-gong bracket were uniform under different levels of excitation, and no obvious rotary and displacement emerged under

low frequency and amplitude. When vibration amplitude rose to 20 mm, the specimen started to wiggle and visible rotary deformation appeared between the connection of the Hua-gong and Ang components. This phenomenon was at its peak under condition 1530 (1.59 Hz of frequency and 30 mm of amplitude) of the specimen. Then, with increased frequency, the whole structure trended toward an organized vibration. No visible friction slip and damage appeared during the whole test.

Dynamic Characteristics of the Specimen

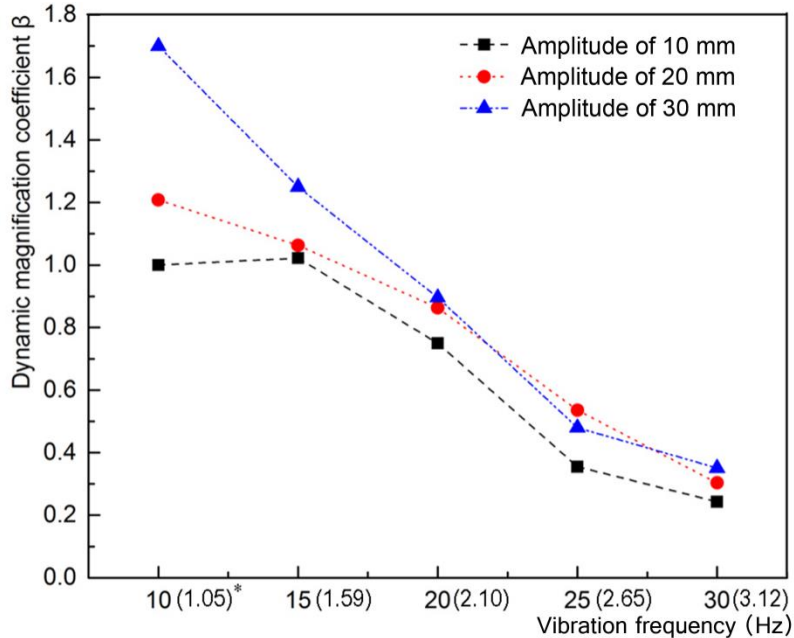
The dynamic magnification coefficient β was acquired according to the ratio of the acceleration response values between the bottom and top of the specimen ($\beta = a_1/a_0$), as shown in Table 3. The anti-seismic design is usually carried out based on seismic intensity, with the peak value of acceleration as an important parameter.

Table 3. The Acceleration and Dynamic Magnification Coefficient

Condition Number	Vibration Excitation (g)	Seismic Intensity	Bottom Acceleration Response a_0 (g)	Top Acceleration Response a_1 (g)	Dynamic Magnification Coefficient β
D1010	0.05	IV	0.052	0.052	1.0
D1020	0.07	IV	0.12	0.145	1.208
D1030	0.12	VII	0.15	0.255	1.7
D1510	0.03	V	0.044	0.045	1.022
D1520	0.10	VII	0.16	0.17	1.063
D1530	0.13	VII	0.16	0.2	1.25
D2010	0.05	VI	0.06	0.045	0.75
D2020	0.18	VIII	0.22	0.19	0.863
D2030	0.23	VIII	0.27	0.242	0.896
D2510	0.07	VI	0.09	0.032	0.355
D2520	0.32	VIII	0.41	0.22	0.536
D2530	0.45	IX	0.50	0.24	0.48
D3010	0.11	VII	0.14	0.034	0.243
D3020	0.55	IX	0.56	0.17	0.303
D3030	0.75	X	0.77	0.27	0.351

However, in this shaking table test the acceleration was calculated by the given vibration frequency and amplitude due to equipment limitations. From the measured results it can be shown that under the same acceleration, with different combinations of frequency and amplitude, the obtained deformations of the Dou-gong specimen were not same. Curves of the dynamic magnification coefficient of the specimen are shown in Fig. 5. In the case of equal amplitudes, the friction among the mortise-tenon joints and different layer members continuously intensified with the increase of frequency, and the dynamic magnification coefficient clearly decreased.

In the case of equal frequency, especially below the value of 1.59 Hz, the value of β showed the amplification in a certain degree with the increase in amplitude. In conditions in which the frequency was higher than 2.10 Hz, changes in amplitude showed little effect on the value of β . Additionally, the effect of amplitude was also related to the vertical load, especially in the low frequency status, which provided sufficient time for the specimen to pendulate. These conditions can rarely be seen in reality.



* Vibration frequency of the motor (shaking table)

Fig. 5. Curves of dynamic magnification coefficient under same amplitudes

Displacement Response of the Test Specimen and Each Layer

The displacement data of specific components of different layers, including the Lu-dou, Nidao-gong, and Man-gong, were selected to discuss the response on the bottom, middle, and top of the Dou-gong model under different vibration conditions. As shown in Fig. 6.1, for conditions under 1.59 Hz and 2.65 Hz, the displacement curves of the components on the bottom, middle, and top were basically synchronous during the vibration process; this suggested that a steady and coupled condition was maintained among the components, and an adequate level of stiffness was maintained for the whole model. As the height increased, the displacement response extent of the main components increased, and the whole displacement stacked up remarkably at the top. Moreover, due to the limited effect of the vertical load to restrict the displacement, the movement of the barycenter along with vibration conditions lagged behind, which provided an opposite force to the displacement of the top layers. Under conditions at the same amplitude, the measured displacement wave of the major components showed obvious characteristics of the sine wave in accordance with the increase in frequency.

The peak of the displacement response appeared under the condition 1530 and then declined evidently as the frequency increased. This result showed that when the vibration frequency rose within limits, the swing of the whole model was limited effectively by friction between layers and a possible compressional deformation among connection joints. In contrast, the displacement of the middle and top layer components slightly tilted to one side when the frequency rose to 25 Hz and higher, indicating that rotation occurred and was intensified in the middle layer of the Dou-gong model with the increase in frequency. It is important to note that the effects of both friction and compressional deformation were crippled by the unloaded vibration to some degree, and partly resulted in an increase of the displacement response on the top layer, rather than amplifications of the dynamic response in actual situations.

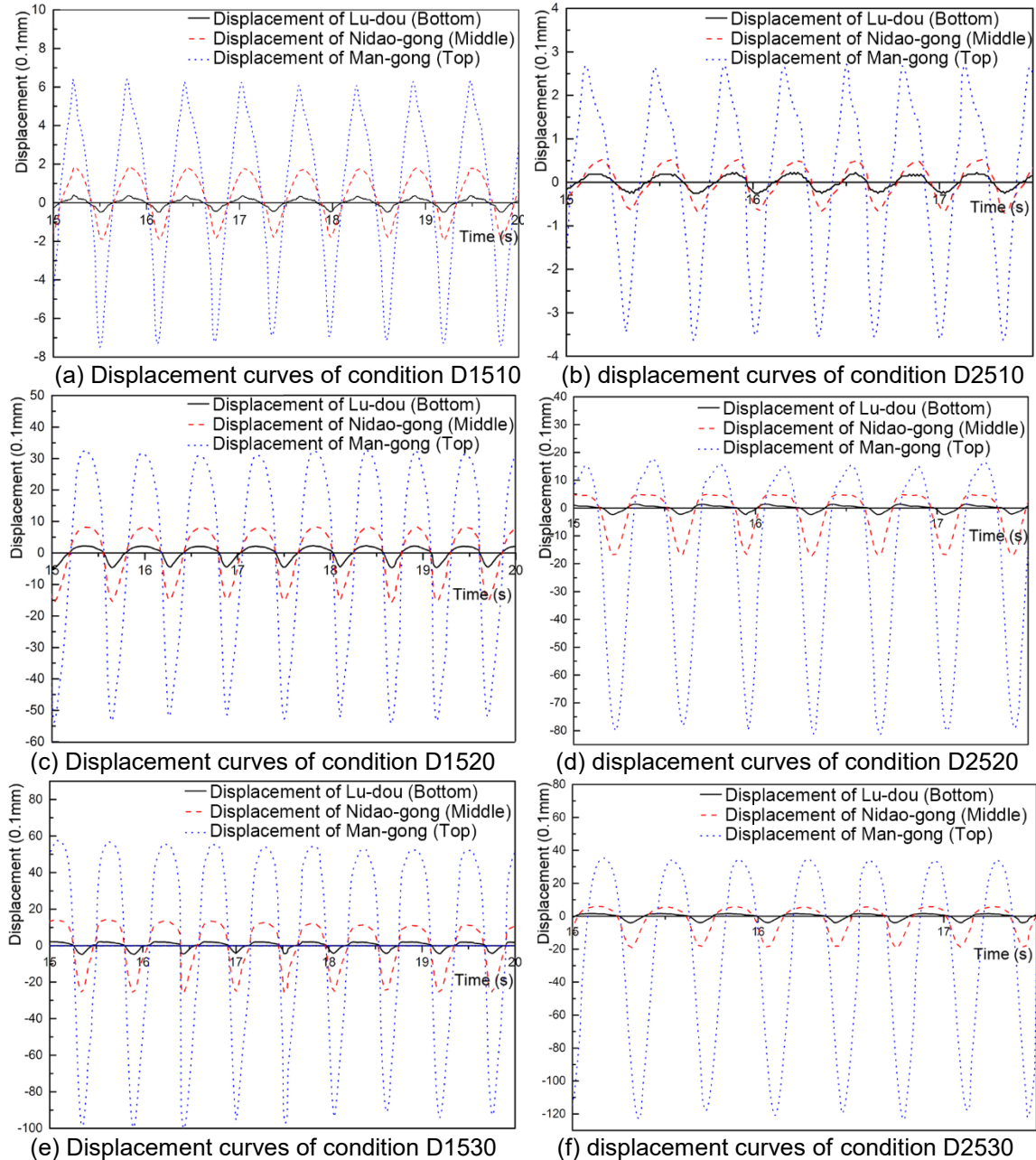


Fig. 6. Curves of displacement under 1.59 Hz and 2.65 Hz

Rotary and Slip Displacement

First, the maximum deformations of the specimen under different conditions were considered. Measured values pertaining to absolute displacement data on top of the specimen were acquired from displacement transducers, while the calculated values were the rotary and slip displacements of the major components synchronized with the measured values and superimposed. The superimposed calculation methods are shown in Fig. 7.

Table 4 shows that the calculated values were basically in agreement with the measured ones; that is, this superimposed calculation method once used in the Dou-gong bracket under the roof load was also suitable for unloaded conditions. Moreover, the rotary

displacement contributed greatly to the maximum values in each condition, and accounted for 87.3% on average.

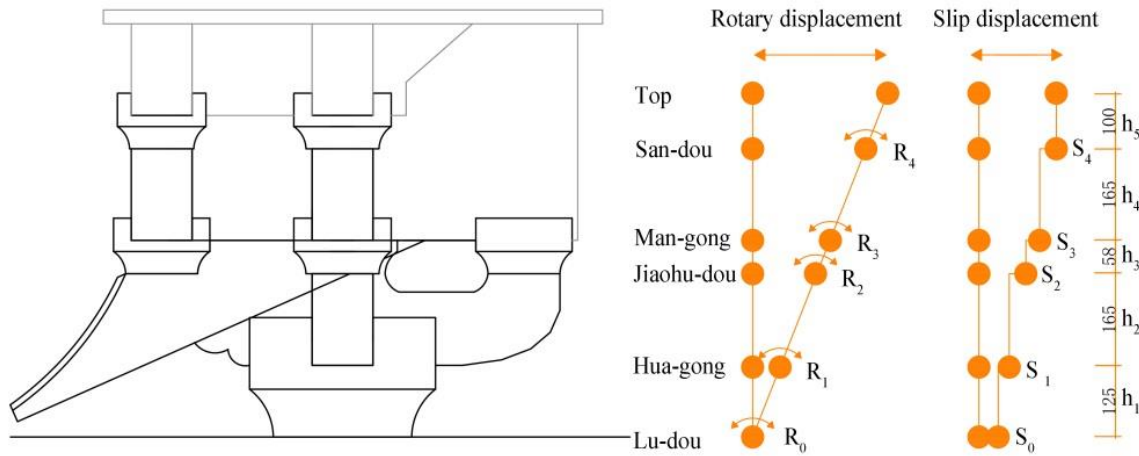


Fig. 7. Rotary and slip deformation of the Dou-gong model

Table 4. Maximum Deformation of the Dou-gong Specimen in Each Condition

Condition	Appear Moment (s)	Measured Value (mm)	Rotary Displacement (mm)	Slip Displacement (mm)	Calculated Value (mm)
D1010	10.59	-0.5625	-0.3608	-0.1134	-0.4742
D1020	3.21	-3.5041	-3.7407	-0.1184	-3.8591
D1030	27.60	-8.2028	-9.6161	0.0513	-9.5648
D1510	25.95	-0.3678	-0.3023	-0.0127	-0.3150
D1520	0.16	-9.1716	-10.0916	0.5802	-9.5114
D1530	14.11	-9.0861	-7.3453	-1.3559	-8.7012
D2010	14.39	-0.2583	-0.2138	0.001	-0.2128
D2020	12.89	3.213	3.4261	-0.249	3.1771
D2030	29.33	-6.332	-5.3322	-1.567	-6.8992
D2510	0.07	0.36	0.2057	0.0034	0.2023
D2520	29.16	-4.0464	-3.4175	-0.2611	-3.6786
D2530	29.30	-3.4602	-2.9923	-0.9825	-3.9748
D3010	27.61	0.9974	0.9932	0.0804	1.0736
D3020	0.42	-9.3558	-7.8601	-1.8439	-9.704
D3030	0.41	-13.2295	-11.212	-2.55	-13.77

Moreover, a comparison of rotary displacement and slip displacement under different combinations of frequencies and amplitudes is shown in Fig. 8. The peak value of rotary displacement fluctuated clearly with the increase of vibration frequency, especially at 1.59 Hz and 3.12 Hz. However, the slip displacement was shown to be more relevant to the amplitude, and the proportion of slip value generally remained at a level of 20% at a 30 mm amplitude, apparently not influenced much by the vibration frequency.

In the set condition D1510, as shown in Table 5, there was a minute time lag on the maximum value of rotary and slip displacement between the whole the Dou-gong specimen and each component, which indicated a strong correlation of deformation that exists between the major sub-units and the whole model. This correlation showed a declining trend from the bottom to the top.

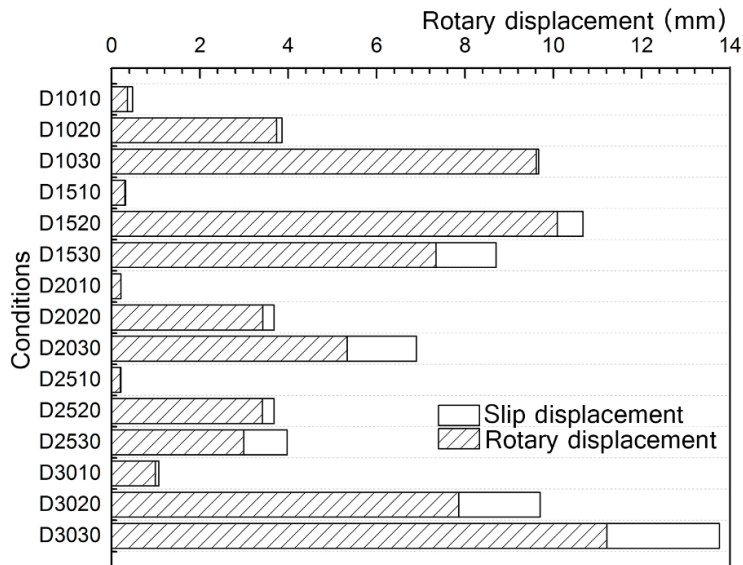


Fig. 8. Rotary and slip displacement of each condition

Table 5. Rotary and Slip Deformation of Major Parts in Condition D1510

Component Name	Rotary Angle (rad)		Slip Displacement (mm)	
	Maximum moment of the model (0.16 s)	Maximum moment of the component (Moment)	Maximum moment of the model (0.16 s)	Maximum moment of the component (Moment)
Lu-dou	-0.00023	-0.00023 (25.95 s)	-0.0937	-0.0976 (25.41 s)
Hua-gong	-0.00052	-0.00053 (26.36 s)	0.0350	-0.0795 (26.12 s]
San-dou on Nidao-gong	-0.00016	-0.00017 (21.06 s)	0.0149	0.0188 (25.93 s)
Qixin-dou	-0.00022	-0.00024 (18.64 s)	-0.0148	-0.0148 (25.95 s)
Man-gong	-0.00039	0.00057 (3.22 s)	0.0274	0.0282 (20.41 s)
San-dou on Man-gong	-0.00018	0.00028 (21.32 s)	-0.0299	-0.0299 (25.95 s)
San-dou on Ling gong	-0.00020	0.00021 (25.92 s)	-0.0468	-0.0468 (25.95 s)

Furthermore, the comparisons of rotary displacement among the main components from bottom to top at the maximum moment of the whole component are shown in Fig. 9. The vibration response showed quite different characteristics along the two axes from the Lu-dou upwards to the top. Axis 1 is the central axis, which contains four measure points—Lu-dou, San-dou on Nidao-gong, Man-gong, and San-dou on Man-gong. Axis 2 is mainly along the Ang components upwards. It contains the Hua-gong with Ang, Qixin-dou, and San-dou on Ling-gong. When the vibration amplitude rose from 10 mm to 20 mm, as can be seen in Figs. 9(a) to 9(b), where the numerical result of rotary displacement increased nearly 10 times, especially for the Lu-dou and Hua-gong components. As the amplitude rose at 30 mm in Fig. 9(c), the rotary displacement of the Lu-dou and Axis 1 tended toward stability, whereas a large deformation still occurred along Axis 2, and the deformation of the Hua-gong with the Ang component accounted for the largest of the whole model all through the test.

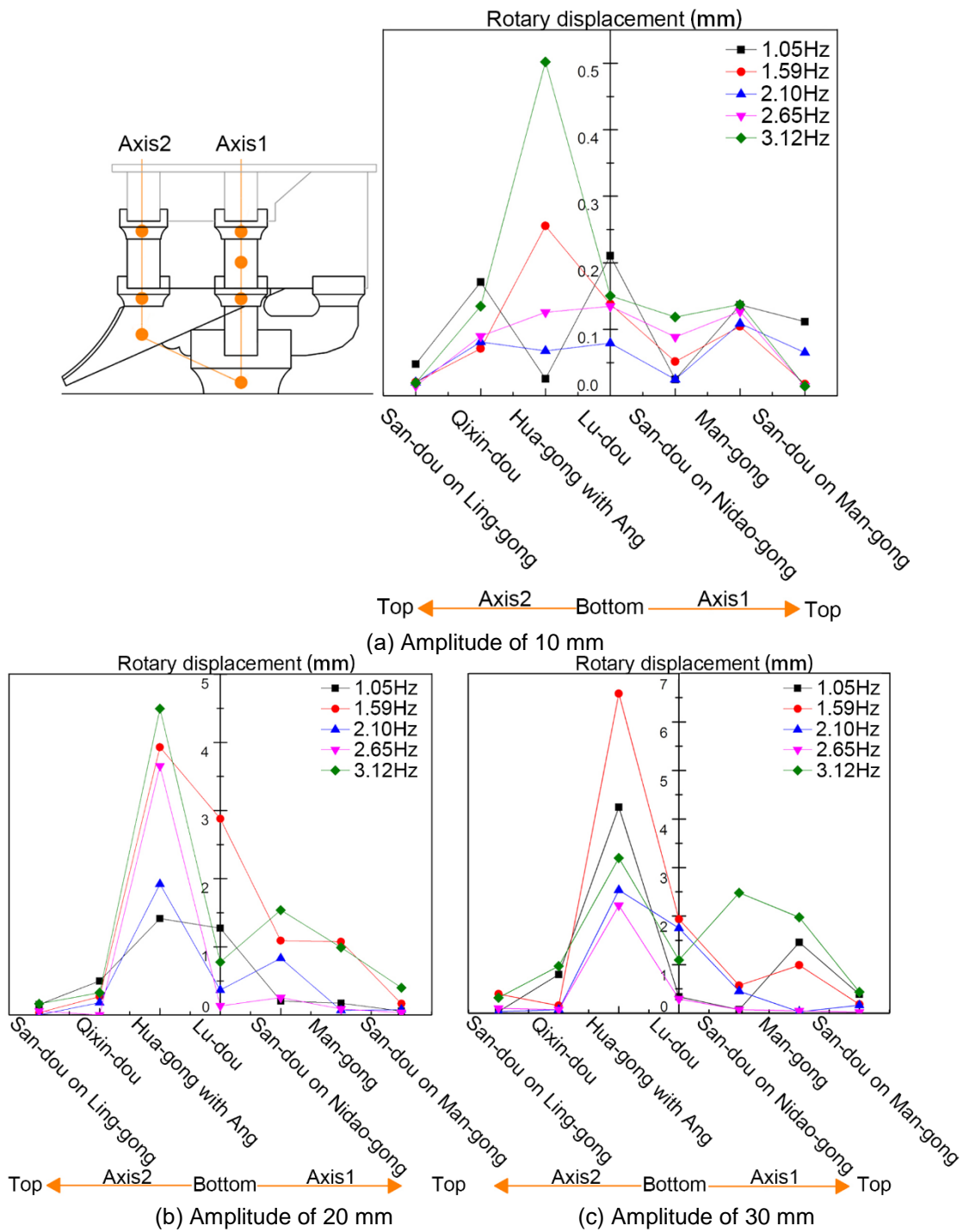


Fig. 9. Rotary displacement of the component along two axes

Under conditions with amplitudes of 20 mm and 30 mm, the proportion of rotary displacement of each member remained roughly stable under different steps of frequency. The Dou-gong specimen was not symmetrical along the vibration direction, and the Lu-dou component was fully fixed to the table, both of which ultimately contributed torsion effects to the Hua-gong with the Ang component. Furthermore, the wooden dowel between the Hua-gong and Ang gave poor support and drawing under strict vibration conditions,

and the different rotary responses along two axes made the whole component susceptible to loss of stability and collapse. The result confirmed that the Hua-gong with Ang component in the later period of the Ming Dynasty started to transform from a structural part to a decoration piece, and this change reduced the cushioning effect of the whole the Dou-gong bracket.

Considering the limitations of the current project, further experiment and analysis should be done under the effect of different level of vertical load. And if possible, the corresponding pseudo static test will be supplemented to give further verification to current conclusions.

CONCLUSIONS

The 15 groups of shaking table tests were performed to investigate the dynamic behavior of the Dou-gong bracket on traditional Chinese wooden structures. A full-scale specimen made of Douglas fir was tested under different conditions of vibration frequency and amplitude and the conclusions drawn from the results are as follows:

1. The Dou-gong bracket system minimizes vibration and impact mainly through the static and sliding friction and rotational energy dissipation between the occlusive components, connected by mortise-tenon joints. To a certain extent, a stronger seismic vibration impact resulted in a more apparent cushioning effect of the Dou-gong bracket.
2. Rotary displacement contributed quite a large part to the maximum deformation of the whole specimen, and it was strongly affected by the vibration frequency. Moreover, the maximum deformation of the whole specimen was strongly related to the maximum deformations of its members, in which the Lu-dou and Hua-gong with Ang components played a leading role.
3. Test results confirmed that the transformation of the Hua-gong with the Ang component in the late Ming Dynasty made it more decorative and decreased its role as a structural member. The asymmetric shape and weak connections led to negative effects of the anti-seismic behavior of the whole system.

ACKNOWLEDGMENTS

The authors are grateful for the support of projects in the National Science & Technology Pillar Program during the Twelfth Five Plan Period No. 2012BAD24B010204; a project funded by the Priority Academic Program Development of Jiangsu Higher Education Institutions (No. PAPD201104); and the National Undergraduate Training Programs for Innovation and Entrepreneurship (No. 201410298016Z).

REFERENCES CITED

- Chen, C. Z. (1955). "The Tianwang palace of Baosheng Temple in Luzhi," *Cultural Relics* 8, 103-110. DOI: 10.13619/j.cnki.cn11-1532/k.1955.08.010
- Chen, Z. Y., Zhu, E. C., and Pan, J. L. (2012). "Mechanics researching advance of Chinese ancient timber structure buildings," *Advances in Mechanics* 42(5), 645-653.

DOI: 10.6052/1000-0992-11-134

- Fan, J., Lv., C., and Zhang, H. (2008). "Study on the time frequency characteristic of ground motions and its effects on structural earthquake response," in: *Proceedings of the 17th National Conference on Structural Engineering*, Wuhan, China, pp. 14-18.
- Fang, D. P., Miyamoto, Y., Iwasaki, S., Deto, H., and Maohong, Y. (1992). "Studies on dynamic and aseismic characteristics of an ancient Chinese timber structure," *Journal of Structural Engineering* 38(3), 951-961.
- Feng, J. L., Zhang, H. Y., Wang, H., and Zhou, H. D. (2009). "Vibration analysis of Dougong layer in ancient timber architectures," *Sichuan Architecture* 29(4), 132-133.
- Gao, D. F., Zhao, H. T., Xue, J. Y., and Zhang, P. C. (2003). "Experimental study on structural behavior of Dougong under the vertical action in Chinese ancient timber structure," *World Earthquake Eng.* 19(3), 56-61. DOI: 1007-6069(2003) 03-0056-06
- GB/T 50165 (1992). "Technical code for maintenance and strengthening of ancient timber buildings," Standardization Administration of China, Beijing, China.
- Kyuke, H., Kusunoki, T., Yamamoto, M., Minewaki, S., and Kibayashi, M. (2008). "Shaking table tests of 'MASUGUMI' used in traditional wooden architectures," in: *Proceedings of the 10th World Conference on Timber Engineering (WCET): Traditional Historic Structures*, Miyazaki, Japan, pp. 300-308.
- Li, T. Y., Wei, J. W., Zhang, S. Y., and Li, S. W. (2004). "Double-parameter seismic damage criterion on wooden structure and seismic response appraisalment on Yingxian wooden tower," *Journal of Building Structures* 25(2), 91-98. DOI: 10.14006/j.jzjgxb.2004.02.015
- Liang, S. C. (1934). "Structural regulations in the Qing dynasty," *Society for the Study of Chinese Architecture*, Beijing, China.
- Pan, J. Z. (2008). *Study on the Anti-seismic Mechanism of Chinese Ancient Timber Structure Buildings*, Ph.D., College Civil Eng., Tongji University, Shanghai, China.
- Shao, Y., Qiu, H. X., Yue, Z., and Chun, Q. (2014). "Experimental study of low-cycle loading test on Song-style and Qing-style dougong," *Building Structure* 44(9), 79-82. DOI: 10.19701/j.jzjg.2014.09.017
- Yuan, J. L., Chen, W., Wang, J., and Shi, Y. (2011). "Experimental research on bracket set models of Yingxian Timber Pagoda," *Journal of Building Structures* 23(7), 66-72. DOI: 10.14006/j.jzjgxb.2011.07.010
- Zhou, Q., Yan, W. M., Guan, H. Z., and Ji, J. B. (2013). "Aseismic behaviors of Tai-he Palace in the Forbidden City," *Journal of Fuzhou University (Natural Science Edition)* 41(4), 487-494. DOI: 10.7631/issn.1000-2243.2013.04.0487
- Zhou, Q., Yan, W. M., and Guan, H. Z. (2015). "Numerical simulation study on structural situation of Tai-he Palace in the Forbidden City," *Building Structure* 45(6), 66-70. DOI: 1002-848X (2015) 06-0066-05

Article submitted: May 31, 2018; Peer review completed: September 29, 2018; Revised version received and accepted: October 18, 2018; Published: October 29, 2018.

DOI: 10.15376/biores.13.4.9079-9091